

Structured light beams constituted of incoming and outgoing waves

Job Mendoza-Hernández* and Maximino Luis Arroyo Carrasco

Facultad de Ciencias Físico -Matemáticas. Benemérita Universidad Autónoma de Puebla, C.P. 72570, Puebla, Pue., México.

Marcelo David Iturbe Castillo and Sabino Chávez-Cerda†

*Instituto Nacional de Astrofísica, Óptica y Electrónica,
Luis Enrique N. 1, 72840 Tonantzintla, Puebla, México*

(Dated: April 27, 2022)

We demonstrate that structured light beams are composed by two traveling waves, and they have the transverse component in direction opposite give us the standing structure in the beam. We represented these waves as incoming and outgoing, respect to the axis of propagation, and they are the complex sum of the two solutions of the transverse component of spatial wave differential equation of the second order. Easily, we can be observed they during the self-healing of the light beam after passing through an obstruction, and with they provide a simple explanation for this property behavior in these. We demonstrated the incoming-wave and outgoing-wave analytic, numerical and experimentally in diffracting beams as the Laguerre-Gauss beams. This representation opens a new way to characterize light beams and offers new insights to understand diffraction phenomena.

PACS numbers: 42.25.Bs

I. INTRODUCTION

The recent Nobel Prize in optical tweezers reflects the importance of structured light beams [1–4]. Structured light beams are beams whose optical properties are tailored to be used in numerous applications [5–7]. It has been demonstrated that some structured light beams have orbital angular momentum, which increases their possible applications [8], such as in classical and quantum communications [9–12], imaging [13], microscopy [14, 15], and micro-manipulation [9]. The spatial and temporal properties of structured light beams are studied with the wave equation, and their approximations, with the Helmholtz equation (HE) or the paraxial Helmholtz equation (PHE) [16–18].

Since the appearance of lasers, Gaussian beams, Hermite-Gauss beams, Laguerre-Gauss beams, and more recently Ince-Gauss beams were generated and described [17, 19]. When these beams have a complex argument, they are called elegant-Hermite-Gauss Beams and elegant-Laguerre-Gauss Beams, respectively [20, 21]. All these beams are described by their transverse distribution as an exact solution of the PHE [16, 22], and they suffer diffraction in propagation.

In the late eighties, the non-diffracting beams, such as the Bessel, Parabolic and Mathieu beams, appeared as solutions of the HE [23–26]. There are other kinds of beams, for example, the accelerating beams which are propagated in parabolic trajectories, known as the Airy beams [27, 28], or solutions proportional to the confluent hyper-geometric function [29, 30]. Also there are beams

that do not have an exact solution of the HE or of the PHE, such as the the Percy beams, which describe the diffraction of a caustic cuspid [31], or the caustic beams [32].

An intriguing property in some structured light beams is their ability of self-healing [23, 33, 34]. This property has applications in microscopy [15], and it even appears in the quantum level [35, 36]. Self-healing occurs when the beams are partially blocked with an opaque object, and after a propagation distance, they recover their transverse intensity distribution. Initially, the self-healing appears in non-diffracting beams [34], and it can be described in terms of conical waves [24, 33, 37, 38]. It can also be described in terms of the Babinet principle [34, 39, 40], and with the relation between two orthogonal field components with attenuated factor[41]. The self-healing property of Laguerre-Gauss beams was recently shown with a property comparison [42]. The structures inside the beams that represented the diffracting beams and non-diffracting beams are described with the first solution of the transverse intensity distribution of HE or PHE; however, the general solution must have two solutions.

The aim of this article is to demonstrate that the structured light beams are constituted by two traveling waves. These waves have their transverse vector in opposite directions, and their sum generates structured light beams as a standing wave. These two fundamental solutions of spatial differential equation of second order are the incoming or outgoing waves. We demonstrate that the Laguerre-Gauss beams have these two waves, with which it is possible to explain the property of self-healing. We give the analytic, numerical and experimental features of these incoming and outgoing waves that constitute the beam. We show that the waves are the complex sum of two solutions of the associated Laguerre differential equation that describes the transverse distribution. The

* job.mendoza@alumno.buap.mx; Present affiliation: Tecnológico de Monterrey, Escuela de Ingeniería y Ciencias, Ave. Eugenio Garza Sada 2501, Monterrey, N.L.64849, (México).

† sabino@inaoep.mx

content of the article includes first, the representation of the general solution for the wave equation and the spatial wave equation in terms of two solutions. Later, we figure out the second solution for the associated Laguerre differential equation that generated the form of the incoming-wave and outgoing-wave. Finally, we present experimental generation of these waves. Both waves are observed in propagation when they are partially blocked.

II. TRAVELING WAVES IN STRUCTURED LIGHT BEAMS

The homogeneous wave equation, Eq. (1), in an homogeneous medium in regions free of currents and charges, is satisfied by a traveling wave $V(\mathbf{r}, t)$ [18, 43].

$$\nabla^2 V - \frac{1}{v^2} \frac{\partial^2 V}{\partial t^2} = 0. \quad (1)$$

The simplest solution of this equation is the traveling plane wave $V = V(\mathbf{r}, \mathbf{s}, t)$, and the general solution is

$$V = V_1(\mathbf{r}, \mathbf{s} - vt) + V_2(\mathbf{r}, \mathbf{s} + vt), \quad (2)$$

where V_1 and V_2 are the two solutions to the equation. These waves are propagated with velocity v , and both waves have opposite direction of plane $\mathbf{r}, \mathbf{s} = cte$.

If the wave could be separated as $V(\mathbf{r}, t) = R[U(r)F(t)]$, where R denotes the real part, and $F(t) = \exp(-i\omega t)$ is a harmonic function, we find that U must satisfy the Helmholtz equation as

$$\nabla^2 U + k^2 U = 0, \quad (3)$$

where $k = \omega/v$ is the wave vector and $U(\mathbf{r}) = A(\mathbf{r})\exp(ig(r))$ is a complex amplitude. The Helmholtz equation, Eq. (3), is the spatial contribution to the wave equation. The general solution depends on the partial differential equation (PDE) that defined the system.

In order to see the spatial contribution of the Eq. 3, we can use the method of separation of variables to split the PDE into a second-order ordinary differential equation (ODE). This is useful for some symmetric system coordinates (e.g. rectangular, cylindrical and spheroidal). Usually, the method works when the PDE is not a product of differential operators in different variables [45]. After getting the second-order ODE for each variable, we can assign a constant and construct a general solution for each equation. In a direct analogy with the wave equation, the spatial wave equation has two solutions with the wave vector transverse components in opposite directions. We call these waves incoming and outgoing waves. Both waves travel in the direction of vector k , with incoming or outgoing direction, respect to the axis of propagation, with the transverse component in opposite directions. The general solution for each second-order ODE can be written as

$$U = U_{in} + U_{out}, \quad (4)$$

where

$$U_{in} = U_1 - iU_2, \quad (5)$$

$$U_{out} = U_1 + iU_2, \quad (6)$$

where U_{in} and U_{out} are the incoming and outgoing waves, and U_1 and U_2 are the two solutions to the second-order ODE.

If the Helmholtz equation wave is written with circular cylindrical symmetry, and the field is separable in the transverse and longitudinal coordinates as $U(\mathbf{r}) = U(r)\exp(ik_z z)$, the incoming and outgoing waves respect to axis z are of the form:

$$U_{in}(r) = U_1(r) - iU_2(r), \quad (7)$$

$$U_{out}(r) = U_1(r) + iU_2(r). \quad (8)$$

In this case, $U_{in}(r)$ and $U_{out}(r)$ are Hankel functions [45]. However, standing waves are almost always used, in which case $U(r) = U_{in}(r) + U_{out} = 2U_1(r)$ is the first solution of the second-order ODE. The simplest case for circular cylindrical symmetry is when $U(r) = 2J_0(k_t r)$, where J_0 is the Bessel beam, k_t is the transverse component, and k_z is the longitudinal component of $k^2 = k_z^2 + k_t^2$. Because the intensity is independent of z , $I(r, z) = I(r, 0)$, they are known as non-diffracting beams [23], and they show the self-healing property [24, 33].

The diffraction beams $I(r, z)$ can be analyzed with the paraxial Helmholtz equation [17, 18], a second-order PDE whose solutions can be found with the method of separation of variables. In circular cylindrical symmetry, these are written as

$$U_{in}(r, z) = U_1(r, z) - iU_2(r, z), \quad (9)$$

$$U_{out}(r, z) = U_1(r, z) + iU_2(r, z), \quad (10)$$

where $U_{in}(r, z)$ and $U_{out}(r, z)$ are the incoming and outgoing waves for paraxial approximation, and $U_1(r, z)$ and $U_2(r, z)$ are the two linear independent solutions. The standing wave for diffracting beams is written as

$$U(r, z) = U_{in}(r, z) + U_{out}(r, z). \quad (11)$$

Equation (11) gives a shape structured by two waves. Therefore, we can easily observe the behavior of the beams when they are propagated and when they are partially obstructed.

III. THE CONSTRUCTION OF INCOMING AND OUTGOING WAVES FOR LGB

The traveling wave solutions that describe the propagation in Laguerre-Gauss beams are found with the solutions of the associated Laguerre differential equation (ALDE).

It is well-known that the LGBs are solutions of the paraxial wave equation in cylindrical coordinates (r, φ, z) [17, 22]. When the method of separation of variables is applied, the ALDE equation appears and governs the radial features, so their first solution is given by the *associated Laguerre polynomial* $L_n^m(x)$ [45, 47–49] (for simplicity in these functions we only use the x coordinate). The parameters n and m are the radial and azimuthal orders of the polynomial with integer values. It is important to highlight that the second solution with n and m integer values is not present in the literature for this reason. In this document, we indicate a way to find it by using the first solution.

In order to find the second solution with n and m integer values, it is useful to use the confluent hypergeometric function (CHF) of first kind $\Phi(a, m; x)$ with a non-integer number [45, 50], where the associated Laguerre polynomial $L_n^m(x)$ [45], can be written as

$$L_n^m(x) = \frac{(m+n)!}{m!n!} \Phi(-n; m+1, x), \quad (12)$$

which is reduced to the associated Laguerre polynomial of degree n when the index sum is $k = n$, and when it is multiplied by $(m+n)!/m!n!$.

A second solution to ALDE is introduced with the function $U(a, m, x)$, the confluent hypergeometric function of the second kind (Tricomi function) [45]. The problem with $\Phi(-a, m+1; x)$ and $U(-a, m+1; x)$ is that they are dependent functions when $m = 0, 1, 2, \dots$ and $a = n = 0, 1, 2, \dots$, are integers.

$$U(-n, m+1, x) = (-1)^n \frac{(m+n)!}{m!} \Phi(-n, m+1, x) \quad (13)$$

However, these functions Φ and U are used to defined a second solution to ALDE, as we see in the next section.

A. X function as second solution and Laguerre-Hankel functions. Analytic form of the incoming and outgoing waves

We define the second solution of the ALDE for m and n integers following the methodology given by Hankel and Weber to find the second solution for the Bessel differential equation [53]. This new function is called X after looking for a symbol that describes the function in the math tables [51, 52].

The function X is defined as [54]:

$$X_a^m(x) = \frac{DU \cos(a\pi) - \Phi}{\sin(a\pi)}, \quad (14)$$

where a is not integer, $m = 0, 1, 2, \dots$, and $D = \frac{m!}{(m+a)!}$. For simplicity, we write U and Φ instead of $U(-a, m+1; x)$ and $\Phi(-a, m+1; x)$, respectively. The function X for both integer indexes m and n is constructed as a Neumann function [45]. When the value of $a \rightarrow n$, the right-hand side of Eq. (14) becomes undefined, and it

approaches a limit. Using L'Hospital's rule, we found that [54]:

$$X_n^m(x) = \lim_{a \rightarrow n} X_a^m(x) = \frac{1}{\pi} \left[(-1)^n \frac{\partial(DU)}{\partial a} - \frac{\partial(\Phi)}{\partial a} \right]_{a=n}, \quad (15)$$

where $X_n^m(x)$ is the second solution of the ALDE for $n = 0, 1, 2, \dots$ and $m = 0, 1, 2, \dots$. The factor $D = \frac{m!}{(m+a)!}$ is necessary in order to have the same amplitude and to compare $X_n^m(x)$ with the function $\Phi(-n, m+1, x)$.

The ALDE's most general solution is given by:

$$y(n, m; x) = A\Phi(-n, m+1; x) + BX_n^m(x), \quad (16)$$

where A and B are constants, and indexes m and n are integers.

If we multiply Φ and X from Eq. (16) by

$$C(n, m) = \frac{(m+n)!}{m!n!}, \quad (17)$$

then $X_n^m = CX_n^m$ and $L_n^m = C\Phi(-n, m+1; x)$.

The solutions X_n^m and L_n^m for the ALDE allow us to define the Hankel type functions as

$$LH_n^m(1; x) = L_n^m(x) + iX_n^m(x), \quad (18)$$

$$LH_n^m(2; x) = L_n^m(x) - iX_n^m(x). \quad (19)$$

Therefore, Eq. (18) and Eq. (19) are **Laguerre-Hankel** functions of the first and second kind. When these functions are together, the Laguerre polynomial function results as

$$[LH_n^m(1; x) + LH_n^m(2; x)] = 2L_n^m(x). \quad (20)$$

The Laguerre-Hankel functions describe the two fundamental functions in the transverse direction for the generation of incoming and outgoing waves.

IV. BEHAVIOR OF INCOMING AND OUTGOING WAVES IN LAGUERRE-GAUSS BEAMS

We consider the definition of Laguerre-Gauss beams LGB as in [22]. The incoming and outgoing waves that constitute the Laguerre-Gauss beam are defined by the Laguerre-Hankel $LH_n^{|m|}$ functions. Also, the X-Gauss beam (XGB) is generated with the function $X_n^{|m|}$ as

$$U_{in,out} = A_0 \frac{w_0}{w(z)} \left(\frac{\sqrt{2}r}{w(z)} \right)^{|m|} LH_n^{|m|} \left(p; \frac{2r^2}{w^2(z)} \right) \times \exp \left[\frac{-r^2}{w^2(z)} - \frac{ikr^2}{2R(z)} + i(2n + |m| + 1)\Phi(z) - im\varphi \right], \quad (21)$$

where $LH_n^{(m)}(p; r)$ is the Laguerre-Hankel function for type $p = 1, 2$, and n and m are the radial and azimuthal indices. The parameters in Eq. (21) are the beam waist w_0 , the beam width $w^2(z) = w_0^2 [1 + (z/L_D)^2]$, the transverse phase front $R(z) = z [1 + (L_D/z)^2]$ and the Gouy phase shift $\Phi(z) = \tan^{-1}(z/L_D)$. In all these expressions $L_D = kw_0^2/2$, is the Rayleigh distance or diffraction distance for the wave number $k = 2\pi/\lambda$.

In order to show the features of the incoming and outgoing waves, we normalized the transverse coordinate to w_0 and the longitudinal coordinate z to L_D in Eq. (21). It is important to note that the explicit solution of X_n^m and complete features will be reported elsewhere.

The main observation of this work is the behavior of LGB in terms of two waves, the incoming and outgoing, and an approach to obtain these waves. Therefore, we approach the function X_n^m taking the nearest integer as $a \rightarrow n$ in the first term of the sum in Eq. (15), taking $k = n$ elements of the series. In the second term of the sum in Eq. (15), we take at least $k = 3n + 1$ elements in the series, in order to have the same number of rings in the XGB and in LGB. In this way, we avoid the divergence on both sides of the function.

Figure 1 shows the central intensity profile of the incoming wave, including the LGB and XGB. The incoming and outgoing waves diverge at the origin because of their logarithmic solutions, since the function X appears in the second solution [45]. We select the intensity in the center of the beams to be at least three times larger than the lobes, in order to observe their contributions. We can observe the relation between LGB and XGB. LGB has a maximum whereas XGB has a minimum. Figure 1 (a) shows the case when $m = 1$ and $n = 3$, while Fig. 1 (b) shows when $m = 5$ and $n = 10$.

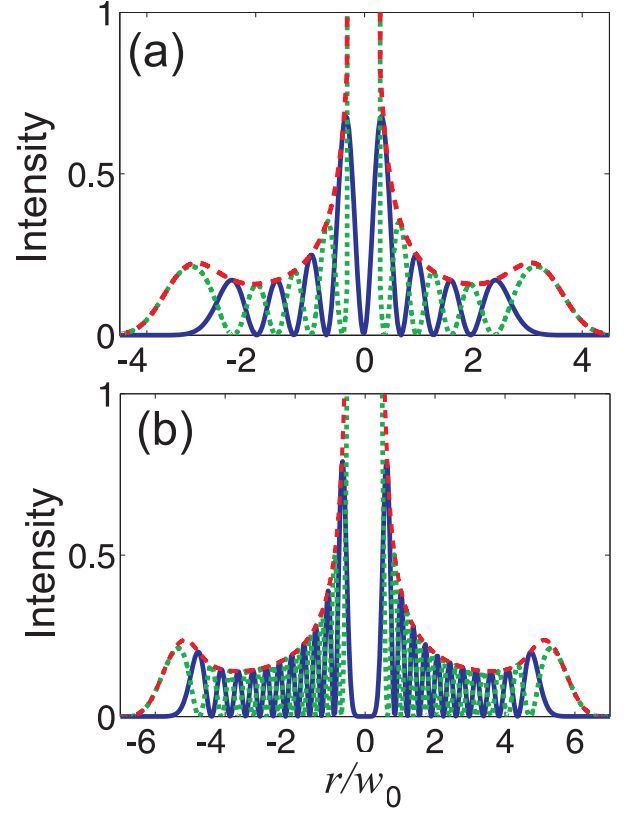


FIG. 1. Intensity profile of the incoming-wave or outgoing-wave (red), LGB (blue), and XGB (green). (a) the case $m = 1$ and $n = 3$, and (b) $m = 5$ and $n = 10$.

The incoming and outgoing waves have a conical wavefront, the first traveling incoming with respect to the axis, and the latter, in the opposite direction. They are shown in Fig. 2. The function $\alpha_{in,out}$ is plotted for each $U_{in,out}$. Figure 2 shows the wavefront for $z = 0$, and $t = 0$. Figure 2(a) shows the case $m = 0$ and $n = 3$, and Fig. 2(b) shows the case $m = 1$ and $n = 3$, mixing the conical and helical wavefronts.

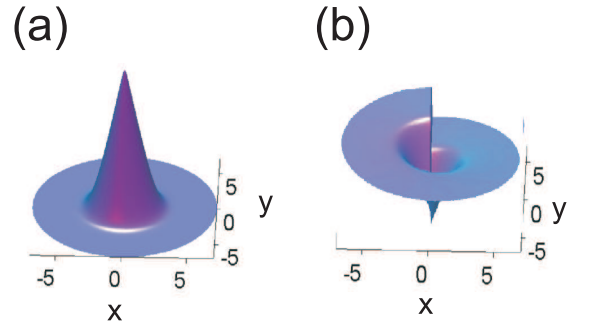


FIG. 2. Conical wavefront for incoming and outgoing waves: (a) without orbital angular momentum $m = 0$, and (b) with orbital angular momentum $m \neq 0$.

The wavefronts of the incoming and outgoing waves help us to understand the self-healing behavior. If the beam is partially blocked by an obstruction of radius a ,

the beam will recover its transverse profile due to the sum of these two waves. The opposite directions of the perpendicular wave vectors hold the stationary distribution after the obstruction (see Fig. 3). The LGB have the conical wavefront, although there is a curve in the conical base in LGB, see the Fig. 3. For the other transverse distributions, the symmetry of the beam may give other surfaces; however, there will be two perpendicular wave vectors with opposite directions in order to hold the shape of the beam.

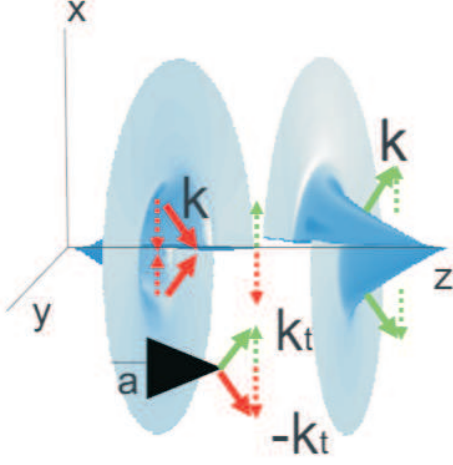


FIG. 3. Wavefronts of incoming and outgoing waves. The direction of transverse wave vector after an obstruction of radius a .

The behavior under propagation of incoming and outgoing waves is shown in Fig. 4. The outgoing wave generates the external part of the LGB, shown in the first row of the figure. The incoming wave presents the internal part of the LGB; this feature acts as an axicon for the generated LGB, such as in the case of Bessel beams[33]. Then, it is possible to consider the generation of optical elements using the incoming wave.

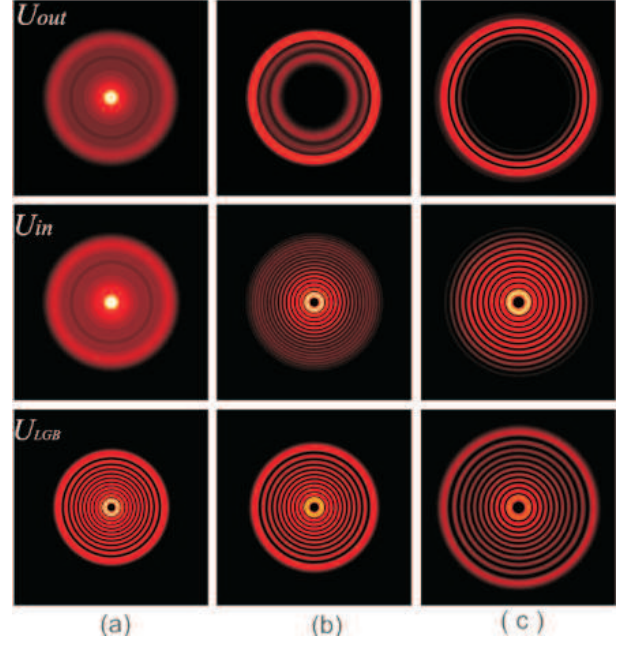


FIG. 4. Stages of propagation of incoming and outgoing waves and LGB: (a) with $m = 5$ and $n = 10$ at the position $z = 0$, (b) $z = 0.5L_D$, and (c) $z = L_D$. The incoming wave is shown in the first row, the outgoing-wave in the second row, and the LGB in the last row.

V. EXPERIMENTAL GENERATION OF INCOMING AND OUTGOING WAVES

We generate experimentally the incoming and outgoing waves, and observed these waves when a Laguerre-Gauss beam is partially blocked. We use the technique developed by Arrizón *et al.* [55]. Figure 5 shows the scheme of setup that we use. We implemented a computer-generated hologram (CH) into an amplitude liquid crystal spatial light modulator SLM (HOLOEYE-LC2002), we use a He-Ne laser (632.8nm) with polarization parallel to the director axis of the SLM. A polarizer is placed after the SLM for to modulate the CH, and eliminated an extra phase. The beam is obtained with a combination of 4f-system and an aperture located at the Fourier plane to decode the wave U . The CCD camera keeps the beam after passing through the second lens f_2 .

We can observed qualitatively the behavior of the incoming and outgoing waves into the Laguerre-Gauss beams when this is partially blocked while they are self-healing, as is shown in the Fig. 6. In order to comparison we observed the behavior also with Bessel beams with the same transverse section and spatial frequency, as in the work done by Mendoza-Hernández *et al.*[42]. Figure 6(a) shows LGB in the first row and BB in the second row partially blocked. Figure 6(b) shows two shadows due to the incoming and outgoing waves: a large low contrast shadow due to the outgoing wave and a small high contrast shadow due to the incoming-wave. The diffracted shadow due to the incoming wave affects the

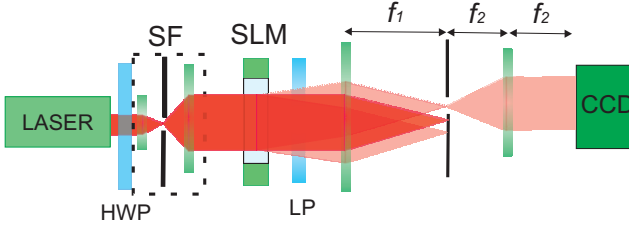


FIG. 5. Experimental scheme for the generation of incoming and outgoing waves U with computer-generated hologram. *HWP*: half wave plate, *SF*: filter system, *P*: polarizer, *SLM*: spatial light modulator, $f_1 = 38\text{cm}$ and $f_2 = 10\text{cm}$ lenses, and *CCD*: camera.

innermost ring and moves around the center of the pattern until it becomes an outgoing wave that increases its size and moves away from the center Fig. 6(c). The LGB has a waist $w_0 = 0.2644\text{mm}$ and a diffraction distance of $L_D = 34.69\text{cm}$ using a lens $f_2 = 10\text{cm}$ into Fig. (5).

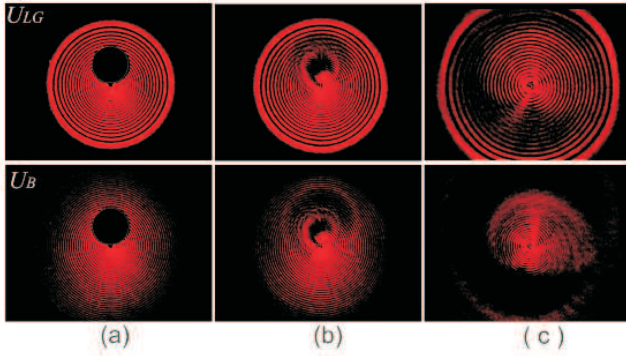


FIG. 6. The self-healing comparison between Laguerre-Gauss beam with azimuthal index $m = 5$ and radial index $n = 19$ and Bessel beam partially obstructed at the position: (a) $z = 0\text{cm}$, (b) $z = 8\text{cm}$, and (c) $z = 34\text{cm}$. We can see the behavior of two shadows due to constitute waves of the beam in (b).

Figure 7 shows the behavior of the partially obstructed incoming and outgoing waves, and also when the LGB is partially blocked. Figure 7 portrays the dynamics of self-healing contained in LGB. The first row presents the large shadow due to the outgoing-wave that diffracts away from the center. In the second row a high contrast shadow is seen due to the incoming wave that affects the innermost ring, which moves around the center. Then, the behavior in partially blocked LGB is caused by two waves that hold the stationary transverse distributions.

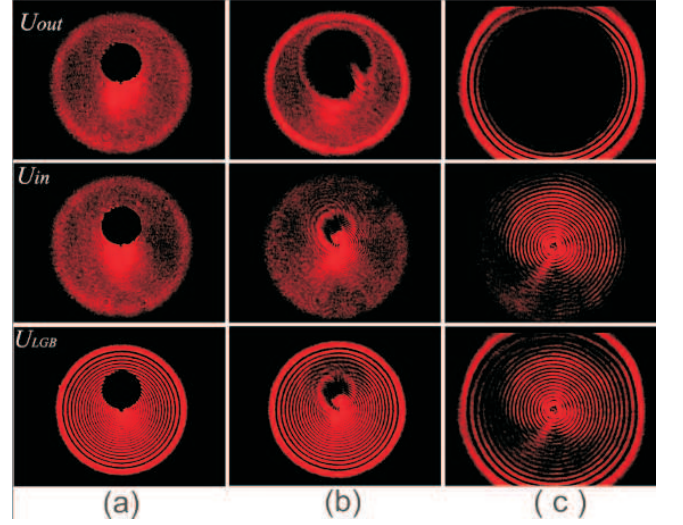


FIG. 7. Incoming and outgoing waves partially obstructed with index azimuthal $m = 5$ and radial $n = 19$ at the position: (a) $z = 0\text{cm}$, (b) $z = 8\text{cm}$, and (c) $z = 34\text{cm}$.

VI. DISCUSSION AND CONCLUSION

It is well known that a solution of the wave equation is a traveling wave equation. However, there are two solutions with the wave vectors pointing in opposite directions. The standing wave is the sum of these two waves and it is the real part of the complex math representation. The spatial feature of the wave is given by the Helmholtz equation, which has two solutions due to the second-order differential equation.

Here we analyzed how these two solutions could give information about the structures of the light beams. The idea is to find the two solutions of the ODE with the boundary conditions appropriate in order to facilitate the solution of the problem. Then, we determined the incoming and outgoing waves, and their transverse components and the axis of propagation of these waves. We explored the problem with circular cylindrical coordinates, in order to compare with the family of non-diffracting beams in the same coordinate system. The standing wave contains the information of the traveling wave, which is observed when the beam is partially blocked under propagation. In this way, we observed their fundamental components, the incoming and outgoing waves.

We established the features of the solutions of incoming and outgoing waves in the Helmholtz and paraxial equations for non-diffracting and diffracting beams. We demonstrated analytically, numerically and experimentally, the incoming and outgoing waves in Laguerre-Gauss beams as diffracting beams. We found the second solution to the associated Laguerre differential equation of radial index integer n and azimuthal index integer m ,

in order to complete the group of solutions essentially for the description of incoming and outgoing waves. These two waves describe the behavior of self-healing in propagating diffracting beams. The transverse structure in the diffracting beams is defined by the standing wave, which is held by the incoming and outgoing waves. The diffractive spreading of the propagation does not change the vision of the two fundamental waves.

ACKNOWLEDGMENTS

Job Mendoza-Hernández acknowledges support from Scholarship CONACYT (Mexico). JMH would like to

thank Victor Arrizon for the summer class about SLM. JMH would like to thank Dorilian Lopez-Mago, Ricardo Tellez-Limon, and Adriana Inclan-Ladino for the discussion on the present work.

-
- [1] A. Ashkin, "Acceleration and Trapping of Particles by Radiation Pressure," *Phys. Rev. Lett.* **24**, 156, (1970).
 - [2] A. Ashkin, and J.M. Dziedzic, "Optical trapping and manipulation of viruses and bacteria," *Science* **235**, 1517-1520 (1987).
 - [3] A. Ashkin, J.M. Dziedzic, and T. Yamane, "Optical trapping and manipulation of single cells using infrared laser beams," *Nature* **330**, 769-771 (1987).
 - [4] A. Ashkin, J.M. Dziedzic, J. E. Bjorkholm, and S. Chu, "Observation of a single-beam gradient force optical trap for dielectric particles," *Opt. Lett.* **11**, 288-290 (1986).
 - [5] L. Allen, S.M. Barnett, and M.J. Padgett (Eds.), *Optical Angular Momentum* (IOP Publishing, 2003).
 - [6] J.P. Torres and L. Torner (Eds.), *Twisted Photons: Applications of Light with Orbital Angular Momentum*, (Wiley-VCH, 2011).
 - [7] D.L. Andrews and M. Babiker (Eds), *The Angular Momentum of Light*, (Cambridge University Press, 2012).
 - [8] L. Allen, M. W. Beijersbergen, R. J. C. Spreeuw, and J. P. Woerdman *Phys. Rev. A* **45**, 8185, (1992)
 - [9] H. Rubinsztein-Dunlop, A. Forbes, M. V. Berry, M. R. Dennis, D. L. Andrews, M. Mansuripur, C. Denz, C. Alpmann, P. Banzer, T. Bauer, E. Karimi, L. Marrucci, M. Padgett, M. Ritsch-Marte, N. M. Litchinitser, N. P. Bigelow, C. Rosales-Guzmán, A. Belmonte, J. P. Torres, T. W. Neely, M. Baker, R. Gordon, A. B. Stilgoe, J. Romero, A. G. White, R. Fickler, A. E. Willner, G. Xie, B. McMorran, A. M. Weiner, "Roadmap on structured light," *J. Optics* **19**, 013001 (2017).
 - [10] M. J. Padgett, "Orbital angular momentum 25 years on," *Opt. Express* **25**, 11265 (2017).
 - [11] J. Wang, J.Y. Yang, I. M. Fazal, N. Ahmed, Y. Yan, H. Huang, Y. Ren, Y. Yue, S. Dolinar, M. Tur, and A. E. Willner, "Terabit free-space data transmission employing orbital angular momentum multiplexing," *Nature Photonics*, **6**, (2012).
 - [12] K. Pang, C. Liu, G. Xie, Y. Ren, Z. Zhao, R. Zhang, Y. Cao, J. Zhao, H. Song, H. Song, L. Li, A. N. Willner, M. Tur, R. W. Boyd, A. E. Willner, "Demonstration of a 10 Mbits quantum communication link by encoding data on two LaguerreGaussian modes with different radial indices," *Opt. Lett.* **43**, (2018).
 - [13] M. J. Padgett, R. W. Boyd, "An introduction to ghost imaging: quantum and classical," *Phil. Trans. R. Soc. A*, **375**, (2017)
 - [14] T. A. Planchon, L. Gao, D. E. Milkie, M. W. Davidson, J. A. Galbraith, C. G. Galbraith, E. Betzig, "Rapid three-dimensional isotropic imaging of living cells using Bessel beam plane illumination," *Nature Meth.* **8**, 417 (2011).
 - [15] F. O. Fahrbach, P. Simon, A. Rohrbach, "Microscopy with self-reconstructing beams," *Nat. Phot.* **4**, 780-785 (2010).
 - [16] G. D. Boyd, H. Kogelnik, "Generalized Confocal Resonator Theory," *Bell Syst. Tech. J.* **41**, 1347-1369 (1962).
 - [17] A. E. Siegman, *Lasers* (University Science Books, 1986).
 - [18] B. E. A. Saleh, M. C. Teich, *Fundamentals of Photonics* (John Wiley and Sons, 1991).
 - [19] M. A. Bandres, and J. C. Gutiérrez-Vega, "Ince-Gaussina beams," *Opt. Lett.* **29**, 144 (2004).
 - [20] A. E. Siegman, "Hermite- gaussian functions of complex argument as optical-beam eigenfunctions," *J. Opt. Soc. Am.* **63**, 1093 (1973).
 - [21] M. A. Bandres, "Elegante Ince-Gaussina beams," *Opt. Lett.* **29**, 1724 (2004).
 - [22] G. J. Gbur, *Mathematical Methods for Optical Physics and Engineering* (Cambridge University Press, 2011).
 - [23] J. Durnin, J. J. Miceli, Jr., and J. H. Eberly, "Diffraction-Free Beams," *Phys. Rev. Lett.* **58**, 1499 (1987).
 - [24] S. Chávez-Cerda, "A new approach to Bessel beams," *J. Mod. Opt.* **46**, 923 (1999).
 - [25] J. C. Gutiérrez-Vega, M. D. Iturbe-Castillo, and S. Chávez-Cerda, "Alternative formulation for invariant optical fields: Mathieu beams," *Opt. Lett.* **25**, 1493 (2000).
 - [26] M. A. Bandres, J. C. Gutiérrez-Vega, and S. Chávez-Cerda, "Parabolic nondiffracting optical wave fields," *Opt. Lett.* **29**, 44 (2004).
 - [27] M. V. Berry, N. L. Balazs, "Nonspreiding wave packets," *Am. J. Phys.* **43**, 264 (1979).
 - [28] G. A. Siviloglou, J. Broky, A. Dogariu, D. N. Christodoulides, "Observation of accelerating Airy beams," *Phys. Rev. Lett.* **99**, 213901 (2007).
 - [29] V. V. Kotlyar, R. V. Skidanov, S. N. Khonina, and V. A. Soifer, "Hypergeometric modes," *Opt. Lett.* **32**, 724, (2007).
 - [30] M. A. Bandres, and J. C. Gutiérrez-Vega, "Circular beams," *Opt. Lett.* **33**, 177 (2008).
 - [31] J. D. Ring, J. Lindberg, A. Mourka, M. Mazilu, K. Dhoulakia, and M. R. Dennis, "Auto-focusing and self-healing

- of Pearcey beams,” *Opt. Express*, **20**, 18955 (2012).
- [32] J. Mendoza-Hernández, M. L. Arroyo Carrasco, M. M. Méndez Otero, S. Chávez-Cerda, M. D. Iturbe Castillo, “New asymmetric propagation invariant beams obtained by amplitude and phase modulation in frequency space,” *J. Mod. Opt.* **61**, S46-S56 (2014).
- [33] M. Anguiano-Morales, M. M. Méndez-Otero, M. D. Iturbe-Castillo, and S. Chávez-Cerda, “Conical dynamics of Bessel beams,” *Opt. Eng.* **46**, 078001 (2007).
- [34] Z. Bouchal, J. Wagner, and M. Chlup, “Self-reconstruction of a distorted nondiffracting beam,” *Opt. Commun.* **151**, 207 (1998).
- [35] M. McLaren, T. Mhlanga, M. J. Padgett, F. S. Roux, and A. Forbes, “Self-healing of quantum entanglement after an obstruction,” *Nat. Commun.* **424**, (2014).
- [36] E. Otte, I. Nape, C. Rosales-Guzmán, A. Vallés, C. Denz, and A. Forbes, “Recovery of nonseparability in self-healing vector Bessel,” *Phys. Review A*, **98**, 053818 (2018).
- [37] S. Chvez-Cerda, G. S. McDonald, G. H. C. New, “Nondiffracting beams: traveling, standing, rotating and spiral waves,” *Opt. Commun.* **123**, 225 (1996).
- [38] J. Rogel-Salazar, H. A. Jiménez-Romero, and S. Chávez-Cerda, “Full characterization of Airy beams under physical principles,” *Phys. Rev. A* **89**, 023807 (2014).
- [39] J. Aiello, G. S. Agarwal, “Wave-optics description of self-healing mechanics in Bessel beams,” *Opt. Lett.*, **39**, 6819 (2014).
- [40] A. Aiello, G. S. Agarwal, M. Paúr, B. Stoklasa, Z. Hradil, Jaroslavreháček, P. de la Hoz, G. Leuchs, L. L. Sánchez-Soto, “Unraveling beam self-healing,” *Opt. Express*, **25**, (2017).
- [41] V. Arrizon, G. Mellado-Villaseor, D. Aguirre-Olivas, H. M. Moya-Cessa, “Mathematical and diffractive modeling of self-healing,” *Opt. Express*, **26**, (2018).
- [42] J. Mendoza-Hernández, M. L. Arroyo Carrasco, M. D. Iturbe Castillo, and S. Chávez-Cerda, “Laguerre-Gauss beams vs Bessel beams showdown: peer comparison,” *Opt. Lett.* **40**, 3739-3742 (2015).
- [43] M. Born, E. Wolf, *Principles of optics. Electromagnetic theory of propagation, interference and diffraction of light*. (Seventh (expanded) edition, Cambridge University Press, 1999).
- [44] N. N. Lebedev, *Special Functions and their Applications* (Dover Publications Inc., 1972).
- [45] G. B. Arfken, and H. J. Weber, *Mathematical Methods for Physicists* (Elsevier Academic Press, Fifth edition, 2001).
- [46] J. Mendoza-Hernández, M. L. Arroyo Carrasco, M. M. Méndez Otero, M. D. Iturbe Castillo, and S. Chávez-Cerda, (Conference paper, Frontiers in optics, Laser Science, Orlando, 2013).
- [47] R. P. Agarwal, D. O. Regan, *Ordinary and Partial Differential Equations. With Special Functions, Fourier Series, and Boundary Value Problems* (Springer, 2009).
- [48] W. F. Trench, *Elementary differential Equations* (Brooks/Cole Thomson Learning, 2000).
- [49] R. K. Nagle, E. B. saff, and A. D. Snider, *Fundamentals of differential equations* (Pearson Addison Wesley, 7th edition, 2008).
- [50] W. W. Bell, *Special functions for scientists and engineers* (Dover Publications Inc., 2004).
- [51] I. S. Gradshteyn, and I. M. Ryzhik. *Table of Integrals, Series, and Products* (Academic Press, 2007).
- [52] M. Abramowitz and I. A. Stegun *Handbook of Mathematical Functions*, (Dover, New York, 1964).
- [53] G. N. Watson, *A Treatise on the Theory of Bessel Function*, (Cambridge at University Press, Cambridge, 1966).
- [54] Job Mendoza-Hernández, PhD thesis, Estudio de la Auto-Reconstrucción de Algunos Campos Estructurados de Luz, “Study of the Self-Healing of some Structured Light Fields”. Benemérita Universidad Autónoma de Puebla, Facultad de Ciencias Físico Matemáticas, Puebla, México (2016).
- [55] V. Arrizón, G. Mendez, D. Sánchez-de-la-llave “Accurate encoding of arbitrary complex fields with amplitude-only liquid crystal spatial light modulators,” *Opt. Express* **13**, 7913-7927 (2005)